www.czasopisma.pan.pl PAN www.journals.pan.pl
Chemical and Process Engineering 2019, 40 (3), 293–304
DOI: 10.24425/cpe.2019.130208

Intensification of free-convection heat transfer in magnetically assisted bioreactor

Maciej Konopacki*, Marian Kordas, Rafał Rakoczy

West Pomeranian University of Technology, Szczecin, Faculty of Chemical Technology and Engineering, Institute of Chemical Engineering and Environmental Protection Processes, al. Piastów 42, 71-065 Szczecin, Poland

The effect of rotating magnetic field on the heat transfer process in a magnetically assisted bioreactor was studied experimentally. Experimental investigations are provided for the explanation of the influence of the rotating magnetic field on natural convection. The heat transfer coefficients and the Nusselt numbers were determined as a function of the product of Grashof and Prandtl dimensionless numbers. Moreover, the comparison of the thermal performance between the tested set-up and a vertical cylinder was carried out. The relative enhancement of heat transfer was characterized by the rate of the relative heat transfer intensification. The study showed that along with the intensity of the magnetic field the heat transfer increased.

Keywords: natural convection, rotating magnetic field; magnetically assisted bioreactor

1. INTRODUCTION

The operation at a distance of a magnetic field (MF) on the fluid has many practical applications. Examples in the chemical engineering include control of the mixing process (Rakoczy et al., 2011; Story et al., 2016), the enhancement of mass transfer process (Rakoczy, 2010a; 2012), the grinding process of a granular material (Rakoczy, 2010b) and many others. Another relevant application area concerns biotechnological processes, in which magnetic fields (MFs) affect cell growth and metabolism (Rakoczy et al., 2016). Practically, bioprocess control is often limited to regulation of temperature at constant values favorable to microbial growth. Therefore, the application of continuously assisted bioprocesses with working volumes entirely surrounded by external MF requires careful heat transfer consideration due to the additional heat generated by the MF system. The effects of MF on heat transfer have received considerable attention by many researches due to its potential in engineering, medical and biotechnological applications. To date, several studies have begun to examine the use of MF in natural convection (Oztop et al., 2009; Pirmohammadi et al., 2009; Rudraiah et al., 1995). The influence of transverse magnetic field (TMF) on free convection was numerically investigated by Al-Najem et al. (1998) and Lo (2010). Nakaharai et al. (2007) studied experimentally the effect of MF on the local and averaged heat transfer of an electrically conducting, turbulent fluid flow. Ceylan et al. (2008) suggested that the magnetic induction may be also a method to introduce thermal energy to the reactor or bioreactor volume.

The main goal of the current study was to determine the effect of a rotating magnetic field (RMF) on the heat transfer in the self-designed magnetically assisted bioreactor (MAB) (Fijałkowski et al., 2016). The MAB

* Corresponding author, e-mail: maciej.konopacki@zut.edu.pl

emits heat during bioprocessing. The maximum temperature of winding during the exposure can reach approximately 70 °C. Therefore, the cooling system for such a magnetically assisted bioreactor should be designed and tested. It should be noticed that most biotechnological processes, e.g. bacterial cellulose production, alcoholic fermentation, are conducted in the temperature of approximately 28 °C (Fijałkowski et al., 2015; Rakoczy et al., 2016). The average heat transfer coefficient from the RMF generator to the liquid was measured by the stabilized heat flow method. The experimental results were generalized by means of dimensionless groups in the form of the relationship between the dimensionless Nusselt number and the product of the dimensionless Grashof and Prandtl numbers.

2. EXPERIMENTAL

A sketch of the experimental set-up is presented in Fig. 1. Briefly, it consists of a housing (1), a RMF generator (2), a container (3), an internal coil (4), a circulating pump (5), an a.c. transistorized inverter (7), a personal computer (8) connected with a temperature signal converter (9). The RMF was generated by the modified 3-phase stator of an induction squirrel cage motor. This RMF generator (2) has three sets of windings, with each phase connected to a different set of windings. In these investigations, the stator was supplied with 50 Hz 3-phase alternating current. The a.c. transistorized inverter (7) was used to adjust the RMF frequency, f_{RMF}, in the range of 10–50 Hz, and to regulate the maximum voltage in the range of 10–100 V. The inverter was connected with a personal computer (8) equipped with the software to control the RMF generator. In the case of the tested set-up, heat was produced in the core by eddy currents that were induced by the RMF. It should be noticed that the heat was produced by the resistance of the windings.

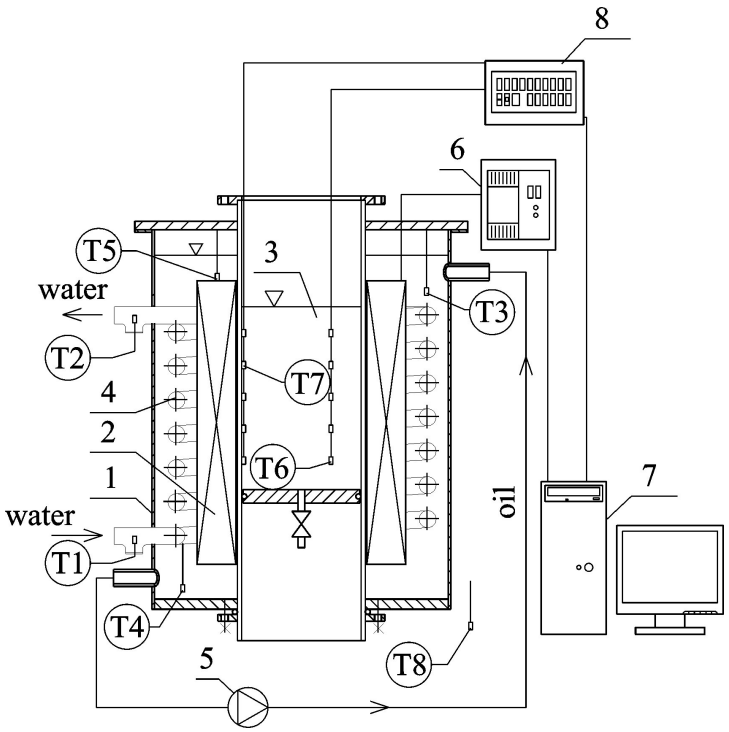

Fig. 1. Sketch of experimental set-up: 1 – housing, 2 – RMF generator, 3 – container, 4 – internal coil, 5 – circulating pump, 6 – AC transistorized inverter, 7 – personal computer, 8 – temperature signal converter, T1–T8 – temperature sensors (where: T1 – cooling water inlet temperature, T2 – cooling water outlet temperature, T3, T4 – oil temperature, T5 – stator temperature, T6 – liquid temperature, T7 – glass container wall temperature, T8 – ambient temperature)

The experimental set-up was supplied with an additional cooling system based on oil circulation. Moreover, the internal coil was placed in the oil to remove the excess of the heat from the experimental system.

The experimental set-up was equipped with a measuring instrument which controlled the temperature of the liquid inside the container (distilled water; volume equal to 4 dm^3) and supervised the real-time acquisition of all the experimental data coming from the sensors. Temperature signals were sampled by special thermal sensors (platinum resistance thermometers Pt100) and were passed through the converter to the personal computer. The experimental investigations were conducted for the steady-state conditions of the heat transfer process. The measured temperature distributions were undertaken to determine the augmentation of the heat transfer by means of the tested device. The experimental set-up with the thermal probe positions is also shown in Fig. 1.

Using the experimental set-up, two cases were analyzed: the heat transfer process without (i) and with (ii) the RMF action. Firstly, the analysis of the heat transfer process without the RMF exposure was based on temperature measurements when the volumetric flow of the working liquid, V_w, (tap water) through the coil was varied in the range between 3 and 15 $dm^3 \cdot min^{-1}$. Secondly, the influence of the RMF on the heat transfer process was analyzed. The water temperature at the inlet of the internal coil was stabilized for both cases (the temperature was equal to 28 °C). The typical temperature profiles for the tested cases and the selected operational conditions are given in Fig. 2.

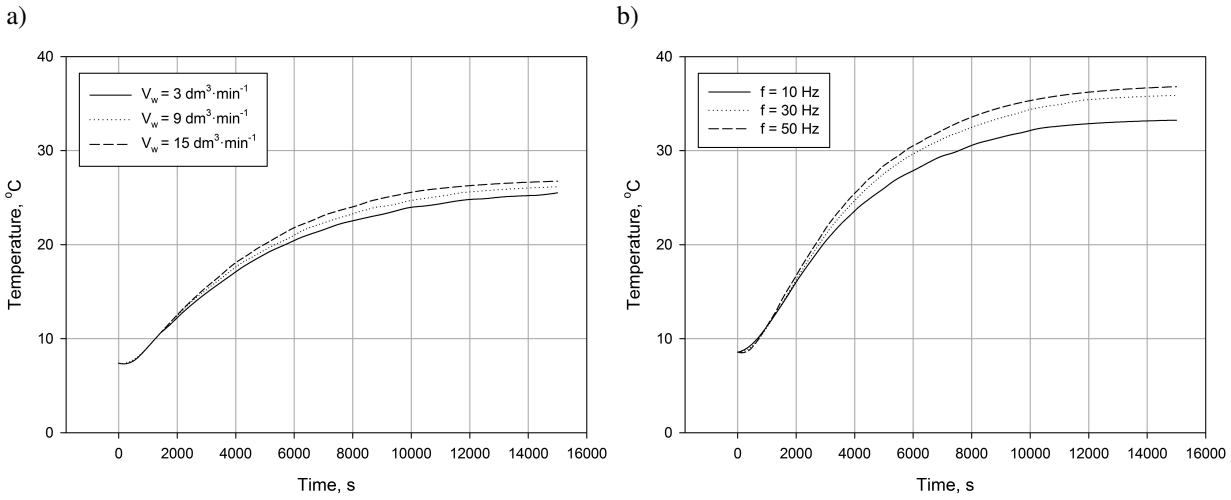

Fig. 2. The typical temperature profiles of culture medium (liquid) for the heat transfer process: a) without the RMF action ($G_w = var$; $f_{RMF} = 0$); b) with the RMF action ($G_w = 9\ dm^3 \cdot min^{-1}$; $f_{RMF} = var$)

The obtained results were used to analyze the radial temperature profiles within the experimental apparatus. The temperature of the fluids as they flow through the magnetically assisted bioreactor (MAB) was not generally constant, but varied over the entire radius, as indicated in Fig. 3.

Figure 3 shows that the areas with the highest heat generation rate produced the most heat and had the highest temperatures. The shape of the profile depends upon the heat transfer coefficient of the various materials or liquids involved. It should be noticed that the heat transfer rate varies along the radius of the MAB because its values depend upon the temperature difference between the hot and cold material or liquid. Moreover, the temperature differential across each material or liquid should be sufficient to transfer the produced heat.

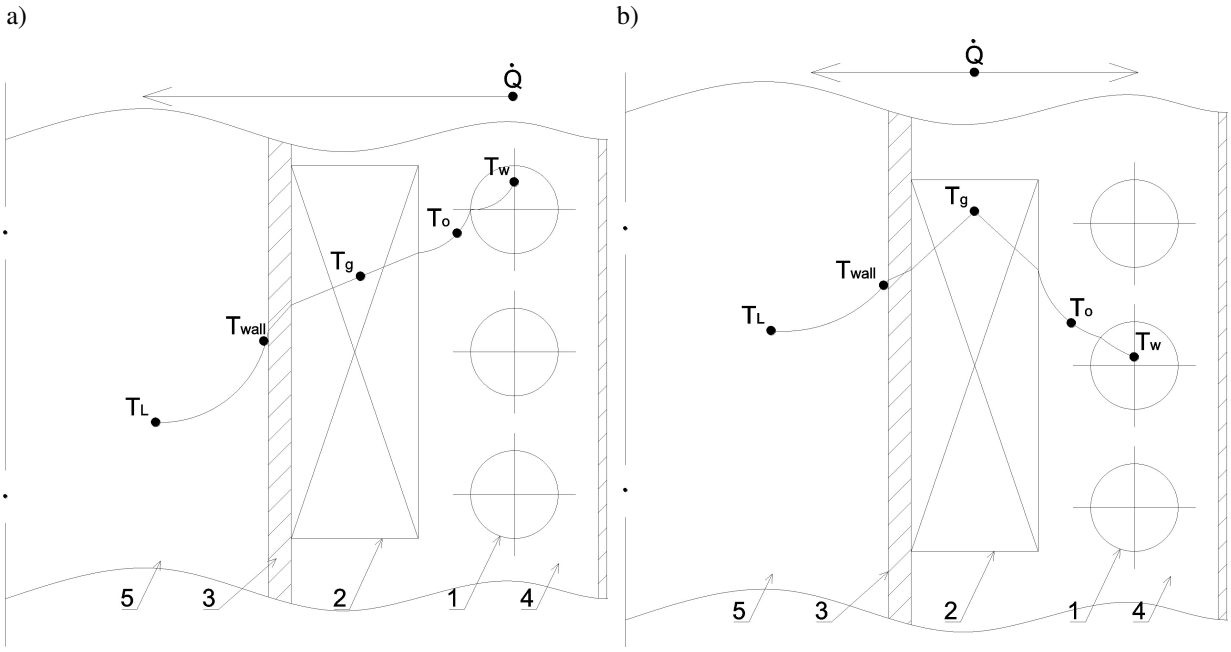

Fig. 3. The radial temperature profiles within the MAB for the heat transfer process: a) without the RMF action; b) with the RMF action. 1 – internal water coil, 2 – generator, 3 – wall, 4 – oil, 5 – liquid (culture medium)

3. RESULTS AND DISCUSSION

In the present work, temperatures were measured at different positions (see Fig. 1) and were used to compute the rate of heat transfer by convection from a surface (or a heat transfer area) at temperature, T_{wall}, to liquid at temperature, T_L (Kothandaraman, 2006).

The heat transfer rate can be calculated from the following equation:

$$\dot{Q}_w = \alpha_w F_c \Delta T_w \tag{1}$$

The temperature difference, ΔT_w, is given by the following relation:

$$\Delta T_w = \int_0^\tau [T_{wall}(\tau) - T_L(\tau)]\, d\tau \tag{2}$$

It should be noticed that the heat transfer rate defined by Eq. (1) should be equalled to the amount of the heat accumulated in the liquid. Consequently, this amount may be expressed by the following relation:

$$\dot{Q}_w = m_w c_p \frac{1}{\tau} \int_0^\tau \left\{ \frac{d\,[T_L(\tau)]}{d\tau} \right\} d\tau \tag{3}$$

The above equations determine the following relation:

$$\alpha_w = \frac{\dot{Q}_w}{F_c \Delta T_w} \quad \Rightarrow \quad \alpha_w = \frac{m_w c_p \dfrac{1}{\tau} \displaystyle\int_0^\tau \left\{ \dfrac{d\,[T_L(\tau)]}{d\tau} \right\} d\tau}{(\pi\, D\, H_L) \displaystyle\int_0^\tau [T_{wall}(\tau) - T_L(\tau)]\, d\tau} \tag{4}$$

The dimensionless Nusselt number is then calculated, taking into consideration the following equation:

$$\mathrm{Nu} = \frac{\alpha_w l}{\lambda_w} \tag{5}$$

For natural convection, in which the fluid motion is not generated by any external source but only by density differences in the fluid occurring due to temperature gradients, the heat transfer coefficient may be defined by means of the following relation (Micheli et al., 2016; Nemati et al., 2012; Piratheepan et al., 2015; Senapati et al., 2016; Spitler et al., 2016; Zhang et al., 2016):

$$\mathrm{Nu} = f(\mathrm{Gr},\ \mathrm{Pr}) \tag{6}$$

From the definitions of the dimensionless Grashof and Prandtl numbers it follows that:

$$\left(\frac{\alpha_w l}{\lambda_w}\right) = f\left[\left(\frac{\beta\, g\, (T_{wall} - T_L)\, D^3}{\nu^2}\right)\left(\frac{c_p\, \eta}{\lambda_w}\right)\right] \tag{7}$$

A comparison of thermal performance between the tested heat transfer cases and the free convection from a heated vertical plate of height can be obtained using the following correlation (Serth et al., 2014):

$$\mathrm{Nu} = \left\{0.825 + \frac{0.387\,(\mathrm{Gr}\,\mathrm{Pr})^{1/6}}{\left[1 + \left(\frac{0.492}{\mathrm{Pr}}\right)^{9/16}\right]^{8/27}}\right\}^2 \tag{8}$$

The heat-transfer coefficient for the case of free convection can be calculated as follows:

$$\left(\frac{\alpha_{th} L}{\lambda_w}\right) = \left\{0.825 + \frac{0.387\,(\mathrm{Gr}\,\mathrm{Pr})^{1/6}}{\left[1 + \left(\frac{0.492}{\mathrm{Pr}}\right)^{9/16}\right]^{8/27}}\right\}^2 \Rightarrow \alpha_{th} = \left\{0.825 + \frac{0.387\,(\mathrm{Gr}\,\mathrm{Pr})^{1/6}}{\left[1 + \left(\frac{0.492}{\mathrm{Pr}}\right)^{9/16}\right]^{8/27}}\right\}^2 \left(\frac{\lambda_w}{L}\right) \tag{9}$$

The above Eq. (8) and Eq. (9) are valid for $0.1 \leq \mathrm{Gr}\,\mathrm{Pr} \leq 10^{12}$ and are accurate to within about ±30%. The characteristic dimension used in the Nusselt and Grashof numbers is the plate length. In these investigations, the plate length was equal to the length of the active part of winding (0.3 m long). The fluid properties are evaluated as the averaged temperature between the fluid temperature in the core and the temperature of plate.

For smaller values of D/L (in the studied case this ratio was 0.5), the effect of surface curvature becomes significant and the following correction factor should be used (the Nusselt number for plate is calculated using Eq. (9))

$$\mathrm{Nu}_{cylinder} = \mathrm{Nu}_{plate}\left[1 + 1.43\left(\frac{L}{D\,\mathrm{Gr}^{0.25}}\right)^{0.9}\right] \tag{10}$$

According to the proposed mathematical description, a plot of data obtained in this work is presented in Fig. 4.

The experimental results shown in Fig. 4 suggest that the heat transfer process in the tested MAB may be analytically described by the following unique function:

$$\mathrm{Nu} = p_1\,(\mathrm{Gr}\,\mathrm{Pr})^{p_2} \tag{11}$$

The constants and exponents were computed by means of the Matlab software and the principle of least squares. It can be seen from Fig. 4 that the experimental data may be approximated for the tested cases by the same type of Equation (11) using various values of the coefficients p_1 and p_2.

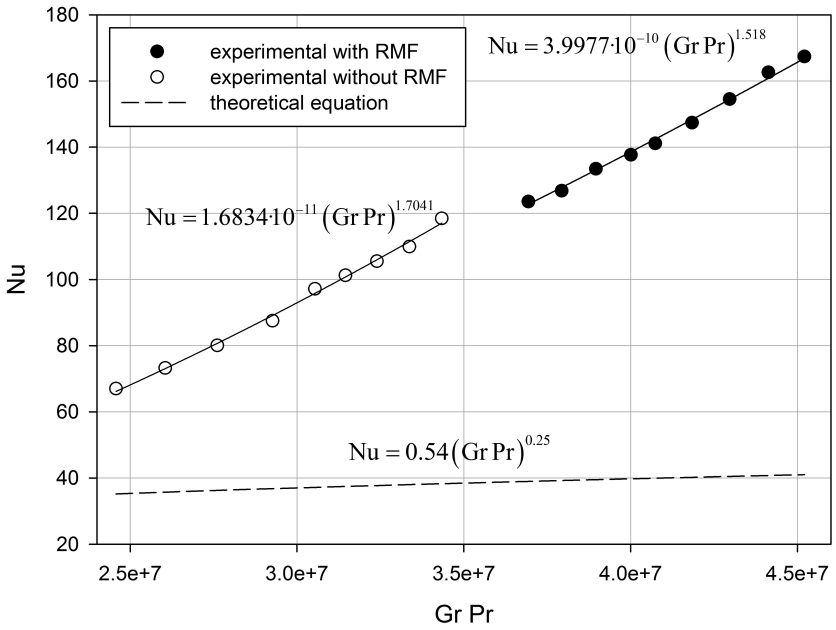

Fig. 4. The dependence $Nu = f(Gr\,Pr)$ for the tested cases (for the heat transfer process with the action of the RMF and without exposure of the RMF)

It can be noticed that the difference between coefficients in the proposed correlations (see Fig. 4) is due to the application of the RMF. Fig. 4 shows that the values of the dimensionless Nusselt number for the heat transfer process under the influence of the RMF are greater than the values of this dimensionless number obtained in this work for heat transfer process without the RMF exposure. This plot also confirms that the volumetric flow of the working liquid (tap water) through the internal coil has a significant effect on the heat transfer rate without the action of the RMF. Generally, the high-volume flow rate is connected with the increase in the dimensionless Nusselt numbers.

According to the obtained data, we can infer that the application of RMF has significant influence on the heat transfer rate. The heat transfer coefficient is on average by about 27% higher under the action of the RMF than without the RMF application.

Figure 4 indicates that significant enhancement in the heat transfer performance for the tested apparatus is obtained with respect to the vertical cylinder. The obtained results indicate that the transfer rate for the MAB is consequently higher than that obtained for the natural convection through a vertical cylinder.

To characterize this relative enhancement in the heat transfer performance we define the rate of the relative heat transfer intensification ε_1, that reflects the increase in the heat transfer coefficient in the tested MAB compared to the heat transfer in the vertical cylinder. This criterion is defined in the following form:

$$\varepsilon_1 = \frac{\alpha_w - \alpha_{th}}{\alpha_w} 100\% \tag{12}$$

This factor is presented in the form of a plot of the criterion ε_1 versus the product of the dimensionless Grashof and Prandtl numbers. Figure 5 demonstrates that the calculated criterion increases with the increase of the mentioned product of the dimensionless parameters. The first conclusion drawn from this graph is that the RMF application increases the criterion values by 40%–60%. The heat transfer without the RMF exposure is connected to the increase in the heat transfer intensification factor by 30%–40%. Moreover, the criterion, ε_2, is defined as follows:

$$\varepsilon_2 = \frac{\alpha_w|_{f=var}}{\alpha_w|_{f=0}} \tag{13}$$

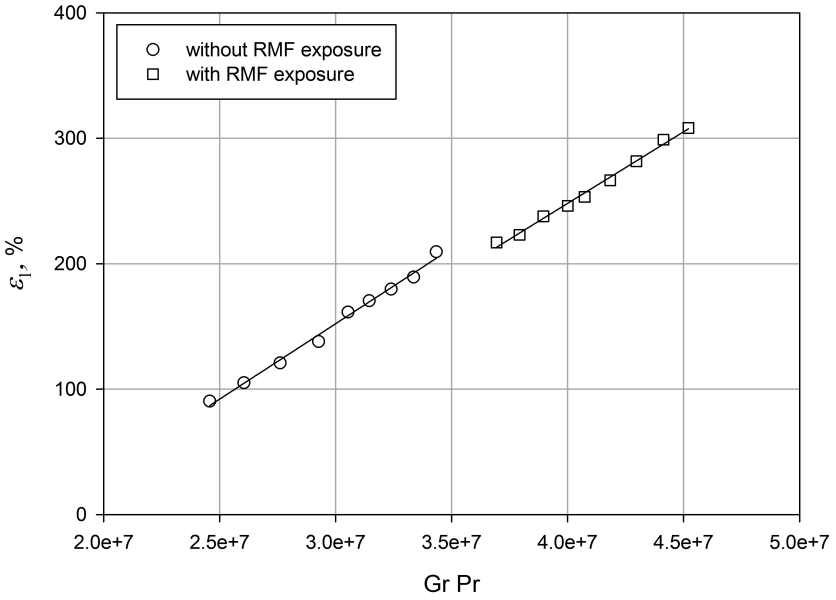

Fig. 5. The comparison of the of the relative heat transfer intensification factor ε_1 for the tested heat transfer cases

It should be noticed that this criterion is calculated for the constant value of the volumetric flow of the working liquid trough the internal coil and the constant temperature at the inlet of the internal coil. This parameter reflects the increase in the heat transfer coefficient for the heat transfer process with the RMF action in comparison to the process without the RMF.

Figure 6 illustrates the obtained relationship (11) as a function of the normalized value of the RMF frequency f^*. This frequency is defined as follows:

$$f^* = \frac{f_{\mathrm{RMF}}}{f_{\mathrm{RMF}}|_{\max}} \quad \Rightarrow \quad f^* = \frac{f_{\mathrm{RMF}}}{50\ \mathrm{Hz}} \tag{14}$$

The results presented in Fig. 6 show that the proposed criterion, ε_2, increases with the normalized values of the RMF frequency f^* and the maximum values of the magnetic induction, $B_{\max}$ The magnetic induction values inside the MAB were detected by means of the microprocessor magnetic induction sensors connected to a Hall probe. The relation between the normalized frequency, f^*, and the maximum values of the magnetic induction, $B_{\max}$, are also presented in Fig. 6.

The experimental results presented in Fig. 6 indicate that the enhancement of heat transfer increases the criterion, ε_2, between about 20% and 70% for the maximum values of the magnetic induction, $B_{\max}$, ranging between 57 and 65 mT.

The area of major importance in bioreactor design involves the heat system for the stable and optimal temperature. Bioreactors are equipped mostly with a stirrer (Choonia et al., 2013; Zhang et al., 2014) or fluid flow systems (Alméras et al., 2016; Hamood-ur-Rehman et al., 2012). Therefore, heat transfer in this apparatus is ruled by the forced convection mechanism. In many cases of bioprocessing, the application of external sources for the generation of fluid motion impair the process. Additionally, as pointed by Fijałkowski et al. (2015) the application of the RMF in the static method of the bacterial cellulose production by *Glucanacetobacter xylinus* requires a strict temperature regime (temperature variation between 28 and 30 °C) without mechanical mixing. Then, the heat transfer process for this case is mostly realized by the natural convection.

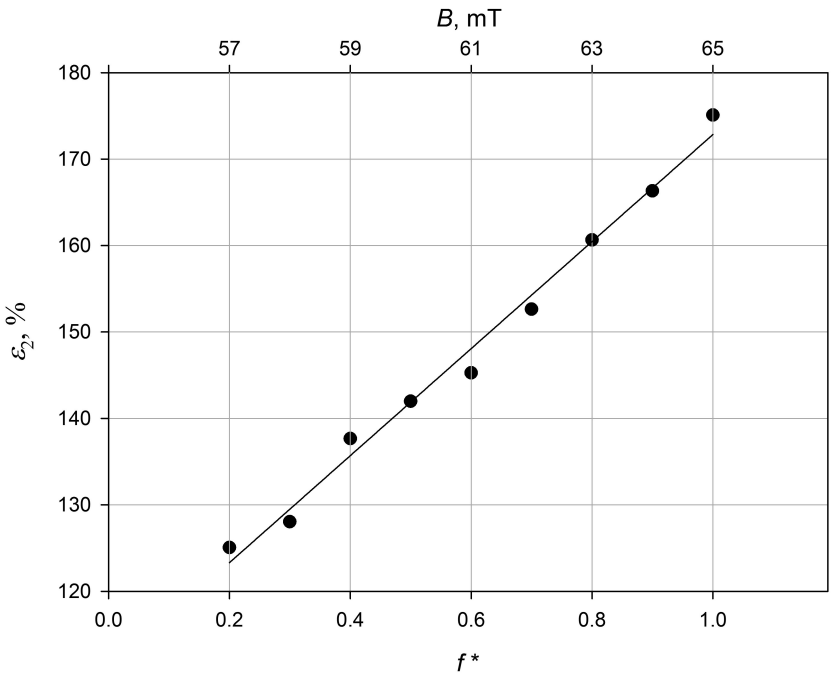

Fig. 6. The rate of relative heat transfer intensification as the function of the normalized value of the RMF (for the volumetric flow through the internal coil $Vw = 9$ dm$^3 \cdot$ min^{-1} and water temperature at the inlet of the internal coil equalled to 28 °C)

The effect of the static magnetic field on natural convection was analyzed for different flow geometry. Moreover, it has been shown that presence of an external magnetic field, especially alternating, can enhance the heat transfer in fluid and this effect can be increased by adding magnetic particles into the fluid (Al-Zamily, 2014; Aminfar et al., 2014; Goharkhah et al., 2015; Kabeel et al., 2015).

The free-convection heat transfer from a heated vertical plate is illustrated in Fig. 7a.

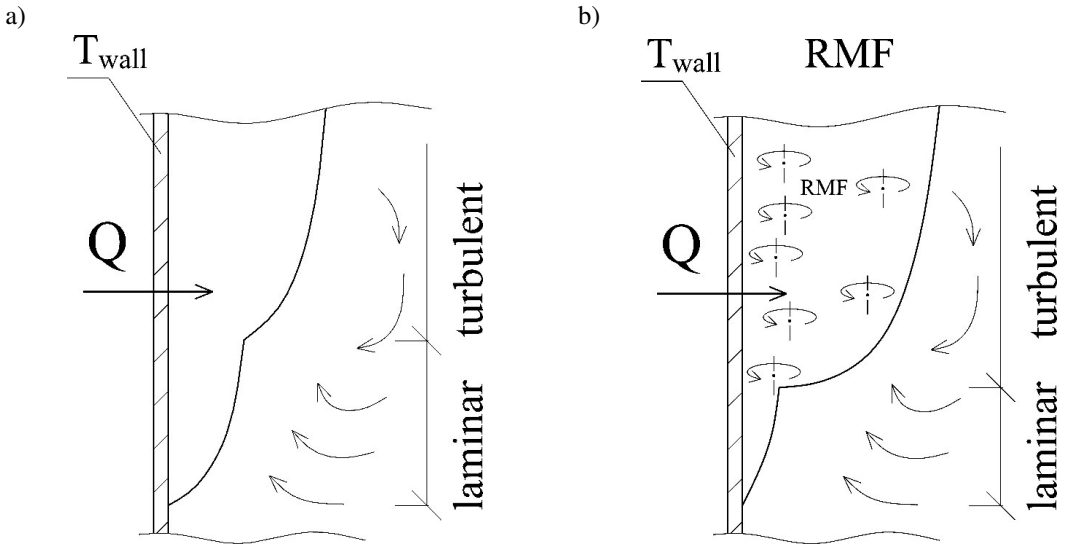

Fig. 7. Free-convection circulation pattern near a heated vertical plate without application of RMF (a) and with the application of RMF (b)

Fluid adjacent to the surface is heated and rises by virtue of its lower density relative to the bulk of the fluid. This rising layer of fluid entrains cooler fluid from the nearly quiescent region further from the heated

surface, so that the mass flow rate of the rising fluid increases with distance along with the plate. Near the bottom of the plate the flow is laminar, but at some point, transition to turbulent flow may occur if the plate is long enough (Serth et al., 2014).

The feature of the RMF is its ability to induce time-averaged azimuthal force which drives the flow of the electrical conducting fluid in the azimuthal direction (Rakoczy, 2010a). In this case, the magnetic field lines rotate horizontally with the rotation frequency of the magnetic field produced. Simultaneously, an electrical field is produced perpendicularly to the magnetic field (Rakoczy et al., 2010). It can be assumed that the external magnetic field acting on the electrically conducting medium may induce virtual loop formation. The magnetic field passing through its enclosed area changes in time during one period of its revolution. According to the induction law, the density of electric current is induced along the virtual loop (Spitzer, 1999). The interaction between current density and the magnetic induction generates the electromagnetic force that drives the culture medium in the direction of the magnetic field rotation. The movement of the fluid exposed to RMF can be explained on the basis of the mentioned microlevel dynamo concept (Hristov et al., 2011). The magnetic field interacting with various charged particles, for example, ions, produces eddy currents in the culture medium (Anton-Leberre, 2010). Eddy currents may generate local magnetic fields around the ions which in combination with an externally-applied magnetic field cause induction of their rotation and thus the movement of the liquid in accordance with the magnetic field. As a consequence of the process, the rotating ions create "dynamos" which cause the effect of micro-mixing (Mehedintu et al., 1997). It should be noticed that this effect may be responsible for increasing heat transfer in the application of RMF. RMF is allowed to generate the turbulent flow by means of the additional mixing on the micro level. Therefore, the incensement of mass flow rate of the rising fluid and the reduction of the laminar flow region near the plate.

4. CONCLUSIONS

An alternative to traditional methods of intensification of biomass production is the use of various types of force fields (e.g., magnetic, electrical, ultrasound). The growth of microorganisms may be stimulated by the use of different types of magnetic fields and it has a number of potential practical applications. The application of MFs is affecting the heat transfer during the MF exposure. In this investigation, the use of RMF in the MAB causing heat transfer was taken into consideration. This process was described by means of the criterions which defined heat transfer intensification under RMF exposure. Practically, these factors may be used to define stable temperature conditions for bioprocessing. Moreover, the proposed mathematical description may be used to compare the influence of different types of magnetic fields on heat transfer operations with respect to bioprocessing.

SYMBOLS

c_p	specific heat of liquid, $\mathrm{J{\cdot}kg^{-1}{\cdot}K^{-1}}$
D	diameter of the container, m
f^*	normalized value of the RMF frequency
F_c	heat transfer area (surface of container), $\mathrm{m^2}$
f_{RMF}	RMF frequency, $\mathrm{s^{-1}}$
Gr	the dimensionless Grashof number
H_L	liquid height in the container, m
l	characteristic length (it is equal to container diameter), m
m_w	mass of the liquid, kg

Nu	the dimensionless Nusselt number
Pr	the dimensionless Prandtl number
Q_w	heat transferred per unit time, W
T_L	temperature of the bulk liquid (see Fig. 3), K
T_{wall}	temperature of the heat transfer area (temperature of container wall, see Fig. 3), K
V_w	volumetric flow rate of liquid, $dm^3 \cdot min^{-1}$
α_w	heat transfer coefficient of the process, $W \cdot m^{-2} \cdot K^{-1}$
ΔT_w	temperature difference between the heat transfer area and the bulk liquid, K
$\varepsilon_{1,2}$	relative heat transfer intensification factors
λ_w	thermal conductivity of liquid, $W \cdot m^{-1} \cdot K^{-1}$
τ	time, s

This study was supported by the National Centre for Research and Development in Poland (Grant No. LIDER/011/221/L-5/13/NCBR/2014).

REFERENCES

Alméras E., Plais C., Euzenat F., Risso F., Roig V., Augier F., 2016. Scalar mixing in bubbly flows: Experimental investigation and diffusivity modelling. *Chem. Eng. Sci.*, 140, 114–122. DOI: 10.1016/j.ces.2015.10.010.

Al-Najem M., Khanafer M.K., El-Refaee M.M., 1998. Numerical study of laminar natural convection in titled enclosure with transverse magnetic field. *Int. J. Numer. Methods Heat Fluid Flow*, 8, 651–672. DOI: 10.1108/09615539810226094.

Al-Zamily A.M.J., 2014. Effect of magnetic field on natural convection in a nanofluid-filled semi-circular enclosure with heat flux source. *Comput. Fluids*, 103, 71–85. DOI: 10.1016/j.compfluid.2014.07.013.

Aminfar H., Mohammadpourfard M., Maroofiazar R., 2014. Experimental study on the effect of magnetic field on critical heat flux of ferrofluid flow boiling in a vertical annulus. *Exp. Therm Fluid Sci.*, 58, 156–169. DOI: 10.1016/j.expthermflusci.2014.06.023.

Anton-Leberre V., Haanappel E., Marsaud N., Trouilh L., Benbadis L., Boucherie H., Massou S., François J.M., 2010. Exposure to high static of pulsed magnetic fields does not affect cellular processes in the yeast *Saccharomyces cerevisiae*. *Bioelectromagnetics* 31, 28–38. DOI: 10.1002/bem.20523.

Ceylan S., Friese C., Lammel Ch., Mazac K., Kirschning A., 2008. Inductive heating for organic synthesis by using functionalized magnetic nanoparticles inside microreactors. *Angew. Chem. Int. Ed.*, 47, 8950–8953. DOI: 10.1002/anie.200801474.

Choonia H.S., Lele S.S., 2013. Kinetic modeling and implementation of superior process strategies for B-galactosidase production during submerged fermentation in a stirred tank bioreactor. *Biochem. Eng. J.*, 77, 49–57. DOI: 10.1016/j.bej.2013.04.021.

Fijałkowski K, Żywicka A., Drozd R., Niemczyk A., Junka A. F., Peitler D., Kordas M., Konopacki M., Szymczyk P., El Fray M., Rakoczy R., 2015. Modification of bacterial cellulose through exposure to the rotating magnetic field. *Carbohydr. Polym.*, 133, 52–60. DOI: 10.1016/j.carbpol.2015.07.011.

Fijałkowski K., Rakoczy R., Żywicka A., Drozd R., Zielińska B., Wenelska K., Cendrowski K., Peitler D., Kordas M., Konopacki M., Mijowska E., 2016. Time dependent influence of rotating magnetic field on bacterial cellulose. *Int. J. Polym. Sci.*, 2016, 1–13. DOI: 10.1155/2016/7536397.

Goharkhah M., Salarian A., Ashjaee M., Shahabadi M., 2015. Convective heat transfer characteristic of magnetite nanofluid under the influence of constant and alternating magnetic field. *Powder Technol.*, 274, 258–267. DOI: 10.1016/j.powtec.2015.01.031.

Hamood-ur-Rehman M., Dahman Y., Ein-Mozaffari F., 2012. Investigation of mixing characteristics in a packed-bed external loop airlift bioreactor using tomography images. *Chem. Eng. J.*, 213, 50–61. DOI: 10.1016/j.cej.2012.09.106.

Hobler T., 1986. *Ruch ciepła i wymienniki*. Wydawnictwo Naukowo-Techniczne, Warszawa.

Hristov J., Perez V. H., 2011. Critical analysis of data concerning *Saccharomyces cerevisiae* free-cell proliferations and fermentations assisted by magnetic and electromagnetic fields. *Int. Rev. Chem. Eng.*, 3, 3–20.

Kabeel A.E., El-Said E.M.S., Dafea S.A., 2015. A review of magnetic field effects on flow and heat transfer in liquids: Present status and future potential for studies and applications. *Renewable Sustainable Energy Rev.*, 45, 830–837. DOI: 10.1016/j.rser.2015.02.029.

Kothandaraman C.P., 2006. *Fundamental of heat and mass transfer*. New Age International (P) Ldt, New Delhi.

Lo D.C., 2010. High-resolution simulations of magnetohydrodynamic free convection in an enclosure with a transverse magnetic field using a velocity-vorticity formulation. *Int. Commun. Heat Mass Transfer*, 37, 514–523. DOI: 10.1016/j.icheatmasstransfer.2009.12.013.

Mehedintu M., Berg H., 1997. Proliferation response of yeast Saccharomyces cerevisiae on electromagnetic field parameters. *Bioelectrochem. Bioenerg.*, 43, 67–70. DOI: 10.1016/S0302-4598(96)05184-7.

Micheli L., Reddy K.S., Mallick T.K., 2016. Thermal effectiveness and mass usage of horizontal micro-fins under natural convection. *Appl. Therm. Eng.*, 97, 39–47. DOI: 10.1016/j.applthermaleng.2015.09.042.

Nakaharai H., Takeuchi J., Yokomine T., Kunugi T., Satake S., Morley N.B., 2007. The influence of a magnetic field on turbulent heat transfer of a high Prandtl number fluid. *Exp. Therm Fluid Sci.*, 32, 23–28. DOI: 10.1016/j.expthermflusci.2007.01.001.

Nemati H., Farhadi M., Sedighi K., Ashorynejad H.R., Fattahi E., 2012. Magnetic field effects on natural convection flow of nanofluid in a rectangular cavity using the Lattice Boltzmann model. *Scientia Iranica*, 19, 303–310. DOI: 10.1016/j.scient.2012.02.016.

Oztop H.F., Oztop M., Varol Y., 2009. Numerical simulation of magnetohydrodynamic buoyancy-induced flow in a non-isothermally heated square enclosure. *Commun. Nonlinear Sci. Numer. Simul.*, 14, 770–778. DOI: 10.1016/j.cnsns.2007.11.005.

Piratheepan M., Anderson T.N., 2015. Natural convection heat transfer in façade integrated solar concentrators. *Sol. Energy*, 122, 271–276. DOI: 10.1016/j.solener.2015.09.008.

Pirmohammadi M., Ghassemi M., Sheikhzadeh G.A., 2009. Effect of a magnetic field on buoyancy-driven convection in differentially heated square cavity. *IEEE Trans. Magn.*, 45, 407–411. DOI: 10.1109/ELT.2008.85.

Rakoczy R., 2010a. Enhancement of solid dissolution process under the influence of rotating magnetic field. *Chem. Eng. Process. Process Intensif.*, 49, 42–50. DOI: 10.1016/j.cep.2009.11.004.

Rakoczy R., 2010b. The application of the informational theory to the analysis of the grinding process under action of transverse rotating magnetic field. *Powder Technol.*, 201, 161–170. DOI: 10.1016/j.powtec.2010.03.021.

Rakoczy R., 2012. Study of effect of temperature gradient on solid dissolution process under action of transverse rotating magnetic field. *AICHE J.*, 58, 1030–1039. DOI: 10.1002/aic.12656.

Rakoczy R., Konopacki M., Fijałkowski K., 2016. The influence of a ferrofluid in the presence of an external rotating magnetic field on the growth rate and cell metabolic activity of a wine yeast strain. *Biochem. Eng. J.*, 109, 43–50. DOI: 10.1016/j.bej.2016.01.002.

Rakoczy R., Masiuk S., 2010. Influence of transverse rotating magnetic field on the enhancement of solid dissolution process. *AIChE J.*, 56, 1416–1433. DOI: 10.1002/aic.12097.

Rakoczy R., Masiuk S., 2011. Studies of a mixing process induced by a transverse rotating magnetic field. *Chem. Eng. Sci.*, 66, 2298–2308. DOI: 10.1016/j.ces.2011.02.021.

Rudraiah N., Barron R.M., Venkatachalappa M., Subbaraya C.K., 1995. Effect of a magnetic field on free convection in a rectangular enclosure. *Int. J. Eng. Sci.*, 33, 1075–1084. DOI: 10.1016/0020-7225(94)00120-9.

Senapati J.R., Dash S.K., Roy S., 2016. Numerical investigation of natural convection heat transfer over annular finned horizontal cylinder. *Int. J. Heat Mass Transfer*, 96, 330–345. DOI: 10.1016/j.ijheatmasstransfer.2016.01.024.

Serth R.W., Lestina T.G., 2014. *Process heat transfer. Principles, applications and rules of thumb*. 2nd ed. Academic Press, USA.

Spitler J.D., Javed S., Ramstad R.K., 2016. Natural convection in groundwater-filled boreholes used as ground heat exchangers. *Appl. Energy*, 164, 352–365. DOI: 10.1016/j.apenergy.2015.11.041.

Spitzer K.H., 1999. Application of rotating magnetic fields in Czochralski crystal growth. *Prog. Cryst. Growth Charact. Mater.*, 38, 59–71. DOI: 10.1016/S0960-8974(99)00008-X.

Story G., Kordas M., Rakoczy R., 2016. Correlations for mixing energy in processes using Rushton turbine mixer. *Chem. Pap. – Chem. Zvesti*, 70, 747–756. DOI: 10.1515/chempap-2016-0008.

Zhang A., Tsang V.L., Korke-Kshirsagar R., Ryll T., 2014. Effects of pH probe lag on bioreactor mixing time estimation. *Process Biochem.*, 49, 913–916. DOI: 10.1016/j.procbio.2014.03.005.

Zhang L., Zhang Y., Zhou Y., Su G.H., Tian W., Qiu S., 2016. COPRA experiments on natural convection heat transfer in a volumetrically heated slice pool with high Rayleigh numbers. *Ann. Nucl. Energy*, 87, 81–88. DOI: 10.1016/j.anucene.2015.08.021.

Received 12 June 2018
Received in revised form 10 July 2019
Accepted 20 August 2019